31st Annual International Conference of the IEEE EMBS
Minneapolis, Minnesota, USA, September 2-6, 2009

Alignment and Elongation of Human Adipose-Derived Stem Cells in Response to Direct-Current Electrical Stimulation

Nina Tandon, Brian Goh, Anna Marsano, Pen-Hsiu Grace Chao, Chrystina Montouri-Sorrentino, Jeffrey Gimble and Gordana Vunjak-Novakovic

***Abstract*— *In vivo*, direct current electric fields are present during embryonic development and wound healing. *In vitro*, direct current (DC) electric fields induce directional cell migration and elongation. For the first time, we demonstrate that cultured human adipose tissue-derived stem cells (hASCs) respond to the presence of direct-current electric fields. Cells were stimulated for 2-4 hours with DC electric fields of 6 V/cm that were similar to those encountered *in vivo* post-injury. Upon stimulation, hASCs were observed to elongate and align perpendicularly to the applied electric field, disassemble gap junctions, and upregulate the expression of genes for connexin-43, thrombomodulin, vascular endothelial growth factor, and fibroblast growth factor. In separate related studies, human epicardial fat-derived stem cells (heASCs) were also observed to align and elongate. It is interesting that the morphological and phenotypic characteristics of mesenchymal stem cells derived both from liposuction aspirates and from cardiac fat can be modulated by direct current electric fields. In further studies, we will quantify the effects of the electrical fields in the context of wound healing.**

I. Introduction

In vivo, direct current electric fields occur during embryonic development [1] and wound healing [2]. *In vitro*, direct current electric fields induce directional cell migration and elongation in a wide variety of cells, including neural cells, keratinocytes, epithelial cells, bone cells, chondrocytes, and fibroblasts [2-7]. The multipotency of adipose-derived stem cells (ASCs) into various lineages such as adipocytes, osteoblasts, and vascular endothelial cells has been widely documented [8], and so the response of ASCs to electric fields is an emerging area of current research [9, 10]. For the first time, we demonstrate that cultured human ASCs respond by morphological and phenotypic changes to direct-current electric fields similar to those encountered *in vivo* post-injury.

Manuscript received April 7, 2009. This work was supported in part by the National Institutes of Health under grants P41 EB002520 and R01 HL076485 and the National Science Council (Taiwan) NSC 97-2221-E-002 -214. NT, AM, and GV-N are with Columbia University, Department of Biomedical Engineering, 622 west 168th Street, Vanderbilt Clinic 12-234 New York NY 10032, emails: nmt2104@columbia.edu, am2085@columbia.edu, gv2131@columbia.edu. PHC is with the Institute of Biomedical Engineering, College of Engineering and College of Medicine, National Taiwan University, 1 Sec. 4, Roosevelt Road, Taipei 10617, Taiwan, email: pgchao@ntu.edu.tw. BG and JG are with Louisiana State University, Pennington Biomedical Research Center, 6400 Perkins Road Baton Rouge, LA 70808, emails: bgoh1@lsu.edu, GimbleJM@pbrc.edu. NT and CM-S are with the Cooper Union for the Advancement of Science and Art, 55 Astor Place, New York, NY 10003, emails: tandon2@cooper.edu, montuo@cooper.edu.

II. Methods

A. Cell Isolation and Culture

Human adipose derived stem cells (hASCs) were isolated from subcutaneous lipoaspirate from donors performing elective surgical procedures (n = 2). The human epicardial adipose tissue-derived ASCs (heASCs) were isolated from epicardial fat surrounding explanted hearts derived from organ transplantation (n = 1). Isolation procedures for both cell types utilized phosphate-buffered saline washes, homogenization and 0.1% Type I collagenase (Worthington Biochemical) digestions. After multiple centrifugations, the stromal vascular fraction was plated and expanded (P1-4) in stromal medium (Dulbecco's Modified Eagle's medium, 10% fetal bovine serum, 1% HEPES, 1% penicillin/streptomycin). Medium was changed three times per week.

For electric field studies, cells (passage 2-4) were plated at 25,000 cells/cm^2 onto sterile glass slides (Fisher Scientific) using removable PDMS (Dow Corning, Sylgard®184) vessels to provide a cell culture surface of dimensions of 5, 1.3, 1 cm (length, width, height, respectively). Prior to cell seeding, culture wells were coated with 0.2% collagen type-I. Cells were plated 14-18 hr prior to insertion into the bioreactor, as previously described [2].

B. Bioreactor Assembly

A modified parallel-plate flow chamber was used to introduce prescribed electric fields to cells cultured on glass

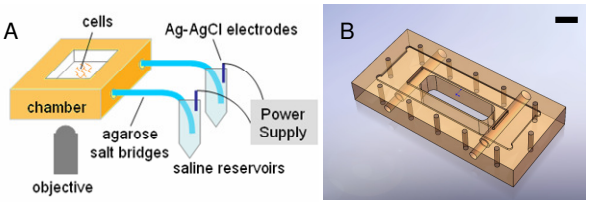

Fig. 1 Experimental Setup for applying direct-current electrical stimulation. (A) The well-defined chamber geometry permits application of a prescribed electrical field strength, and two salt bridges prevent electrolysis products from contaminating the chamber by providing a pathway for current from each media reservoir to an Ag–AgCl electrode (one anode, one cathode). (B) A view of an assembled chamber. Scale bar corresponds to 1 cm.

slides [3, 11], (**Fig. 1A**). In this modification, the tubing that provides fluid flow into and out of the bioreactor is replaced with two salt bridges that provide a conducting pathway for the applied current. One plate of this chamber consists of a machineable, sterilizable polycarbonate block with a glass window, whereas a glass slide with cultured cells represents the second plate (**Fig. 1B**).

The two plates were separated by a uniform-thickness rectangular silicone spacer (McMaster-Carr) with a central rectangular opening, held together with screws and a plastic lid (having a rectangular opening to accommodate the microscope objective). When this chamber is closed properly (tightly enough to prevent leaking, but without cracking the glass slide), a sealed rectangular channel with dimensions of 5, 1.3, 0.250 cm (length, width and height or gap distance, respectively) is created. This well-defined chamber geometry prevents any fluid flow and permits the electric field strength or current density to be calculated from the applied current [3]. Silver–silver chloride electrodes were fashioned out of gauge 23 (0.025") silver wire, as previously described [3, 11], and interfaced with luer ports on each side of the galvanotaxis channel via a pair of 35 cm long, 2 % (weight/volume) agarose–saline bridges. The resistance of the chamber was measured to be ~8 kΩ, which is consistent with theoretical calculations derived from the conductivity of the medium and chamber geometry [3].

C. Electrical Stimulation

Cells were placed into the bioreactor, and stimulated continuously for either 2 or 4 hours by a system maintaining constant current (Keithley SourceMeter 2410) of 3 mA (corresponding to a field strength of 6 V/cm) [3], while maintained in a 37 ˚C, 5% CO_2 incubator.

D. Assessments

For morphometric analysis, bright-field images taken at 10x magnification were analyzed by tracing cell outlines using ImageJ software. The length of the major axis of the cell was used to measure cell length, and the corresponding angle as the angle of orientation of the cell. 30-50 cells were measured in each of 8-10 images from 2-4 separate experiments. Statistical difference for cell length and orientation angle was determined via one-way ANOVA, or f-test, respectively ($p<0.01$ considered significant).

For immunohistochemistry, cells were fixed in 2% formalin, and immunostained for connexin-43 (to monitor gap junction density) and phalloidin (F-actin). For gap junctional analysis, we applied our custom software, as previously described, [11] to images of fluorescently-Cx-43-stained cells. Statistical difference for gap junctional density was determined via one-way ANOVA, ($p<0.01$ considered significant).

For real time polymerase chain reaction (rt-PCR), cells were harvested from the slides with a cell scraper, transferred into Trizol and stored at –80 ^{o}C until analysis. Total RNA was isolated and purified using 1-bromo-3-chloropropane, BCP

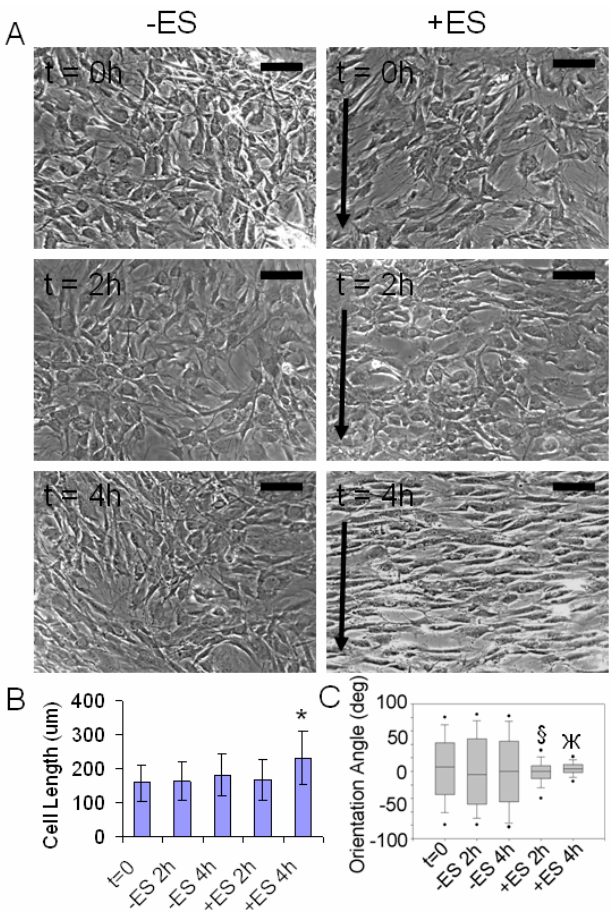

Fig. 2 Morphological changes associated with direct-current stimulation. (A) bright-field images taken at time 0, 2, and 4 hrs for hASCs either unstimulated (-ES) or exposed to an electric field of 6 V/cm (+ES) for 2 or 4 hrs. Scale bar corresponds to 200 um, and arrows correspond to direction of electric field. (B) Average cell length. (C) Orientation angle of cells with respect to the horizontal axis. * Significantly different mean value from all other groups; Ж significantly different variance from all other groups; § significantly different variance from unstimulated controls ($p < 0.01$)

(Molecular Research Center). 2µg of RNA was then reversely transcribed using Moloney Murine Leukemia Virus Reverse Transcriptase (MMLV-RT; Promega) with Oligo dT at 42 ˚C for 1 hour in a 20µl working volume.

Primers for the selected genes were designed using Primer Express (Applied Biosystems). Real time PCR was performed using the SYBR® Green PCR Master Mix (Applied Biosystems) on the 7900 real time PCR system (Applied Biosystems). Universal cycling conditions of 95 °C for 10 min and 40 two step cycles consisting of 95°C for 15 sec followed by 60 °C for 1 min were used. Genes of interest were normalized against *Cyclophilin B*. All RT-PCR assays were performed in triplicate and the *Cyclophilin B*-normalized ratio

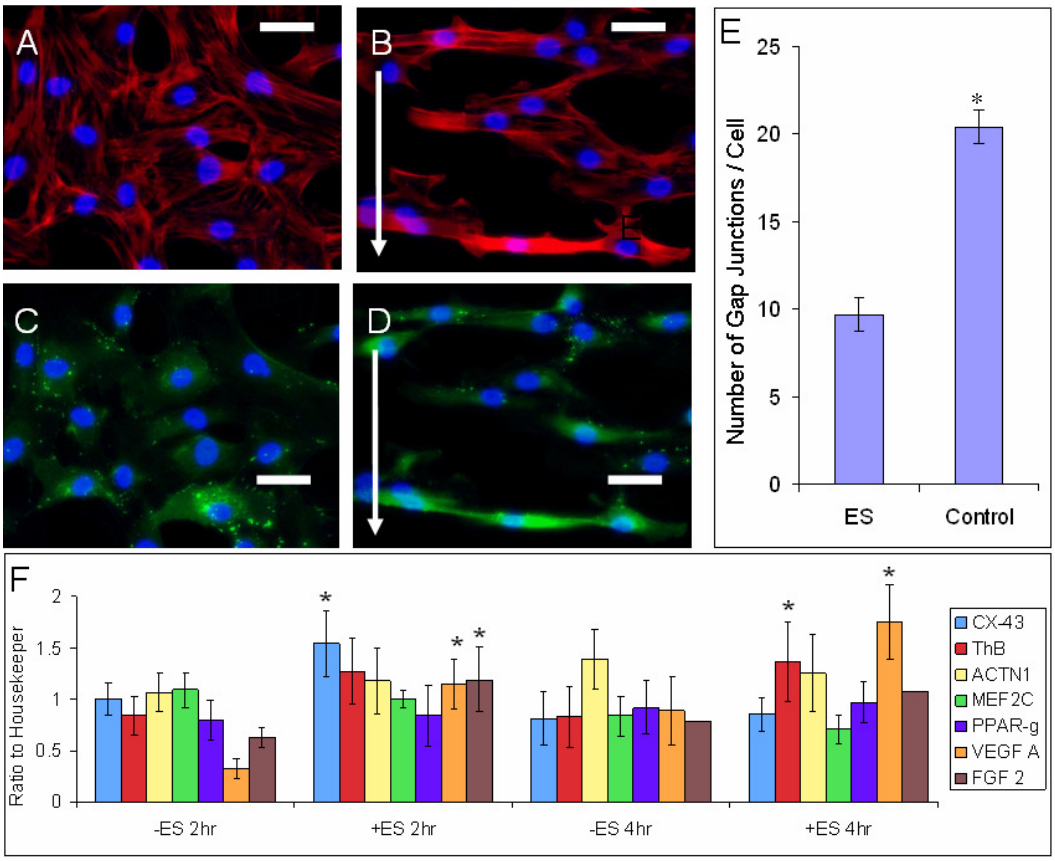

Fig. 3 Ultrastructural and phenotypic changes associated with direct-current stimulation of hASCs. Flourescent images taken at time 0 (A, C) and 4 h (B,D) of cells immunostained for actin with phalloidin (red) (A, B) and connexin-43 (green) (C, D) and DAPI (A-D), for cells either unstimulated (A, C) or stimulated with an electric field of 6 V/cm for 4 h (B, D). Scale bar corresponds to 100um, and arrows indicate the direction of the electric field. (E) Density of gap junctions ($p<0.01$). (F) Gene expression results for RNA levels as compared to housekeeper gene (Cyclo-B) (* $p<0.05$).

data presented in the figures represents the mean ± standard deviation. For this study, the genes of interest were: connexin-43 (Cx-43), thrombomodulin (ThB), actinin alpha 1 (ACTN1), vascular endothelial growth factor (VEGF), myocyte enhancer factor 2C (MEF2C), peroxisome proliferator-activated receptor gamma (PPAR-g), basic fibroblast growth factor 2 (FGF2), osteopontin (OPN). Statistical significance was determined from samples from 3 separate experiments via Mann-Whitney U-test ($p<0.05$ considered significant).

III. RESULTS

A. *Morphology*

hASCs demonstrate a number of morphological changes with the application of the DC stimulus (**Fig. 2A**). By comparing box plots of cells analyzed for various conditions of stimulation, we oberved that the initial, high variance of cell angle (indicating random orientation of the cells) decreases within 2 hours of the onset of stimulation (indicating non-random cell alignment) with a direction perpendicular to the applied electric field (**Fig. 2C**). This alignment becomes more pronounced after 4 hours. At that time, the cells' length increased by 45% (**Fig. 2B**) relative to their length at the onset of stimulation (230 vs. 159 µm, respectively).

Electrical stimulation also appears to result in disassembly of gap junctions and alignment of actin stress fibers (**Fig. 3**). Immunofluorescence microscopy reveals that electrically stimulated hASCs exhibit approximately half the number of gap junctions per nucleus when compared to non-stimulated cells (+ES = 9.67 ± 0.94, -ES = 20.45 ± 0.96).

B. *Gene expression*

hASCs also demonstrate a number of phenotypical changes with the application of the DC stimulus (**Fig. 3F**). After 2 hours of stimulation, cells upregulate genes for connexin-43 (Cx-43), vascular endothelial growth factor (VEGF) and fibroblast growth factor (FGF). After 4 hours of stimulation,

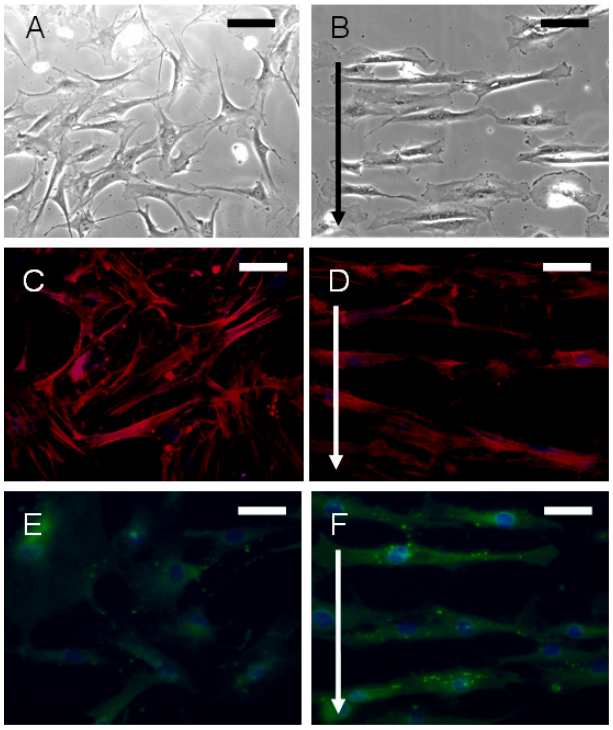

Fig. 4 Preliminary results with electrical stimulation and epicardial adipose-derived heASCs. Bright-field images (A,B), Flourescent images taken of cells immunostained for actin with phalloidin (red) (C, D), connexin-43 (green) (E, F) and DAPI (C-F), for cells either unstimulated (A, C, E) or stimulated with an electric field of 6 V/cm for 4 h (B, D, F). Scale bar corresponds to 100um, and arrows indicate the direction of the electric field.

cells upregulated genes for VEGF and thrombomodulin (ThB).

C. Human epicardial adipose tissue-derived stem cells (heASCs)

In preliminary experiments applying the same protocol to human epicardial-fat derived ASCs as applied to subcutaneous lipoaspirate-derived ASCs, cells exhibited similar alignment of actin fibers, elongation of cells, and disassembly of gap junctions (**Fig. 4**).

IV. DISCUSSION

A. Morphology

In the present investigation, we report for the first time that cultured hASCs exhibit elongation and alignment when exposed to DC electric fields demonstrated previously to elicit galvanotropism in other cell types. We believe that the applied electric field is the primary stimulation in this study, given the lack of bulk fluid flow in the system (fluid rates generated by electro-osmosis in the present study are estimated to be only ~1–15 μm/s in the direction of the cathode [3]) and based on the results of others showing that adding a medium cross-flow did not alter the response to the applied electric field [12, 13]. Additionally, no effect of Joule heating was observed, consistent with past studies [3], which may be attributed to the high resistance associated with the chamber and rapid heat dissipation between the two large parallel glass surfaces containing the cells.

In this study, hASCs demonstrated alignment in a direction perpendicular to the applied electric field within 2 hours of the onset of stimulation, consistent with reports of others applying identical culture conditions to fibroblasts and chondrocytes [2, 3]. Interestingly, our cell elongation-alignment results match those of other studies with hASCs and pulsatile electric field stimuli, in which alignment perpendicular to the applied electric field was observed over the course of days of stimulation [9, 10], as opposed to hours in the current experiment.

In addition, others have noted that monolayers of cells in DC fields respond with more sensitivity than sparse populations of cells [2], perhaps because the latter experience a smaller voltage drop across the width of each individual cell, while the former experience the electric field as a voltage drop across the width of several adjacent, contacting cells communicating via gap junctions. Cells have been suggested, as in the case of substrate stretching studies, to minimize the strain or stress gradient by aligning their long axis perpendicular to the principal direction of stretch. In a similar manner, the cell elongation and perpendicular alignment observed in the current study may be indicative of a mechanism to minimize the electric field gradient across the cell [6].

It is also interesting to note that heASCs and hASCs exhibited such similarity in their morphological changes, even though *in vivo* the heASCs are subjected to pulsatile electric field stimuli due to their close proximity to the heart, the body's largest bioelectrical source, and hASCs are not.

B. Gene expression

DC electric fields are a well-documented biophysical cue for differentiation [1], but given the little-known response of ASCs to electric stimuli, as well as the multipotency of these cells [8], we chose to examine a variety of types of genes in this study. The upregulation of ThB, VEGF and FGF, in combination with the lack of upregulation of OPN, might indicate a decrease of osteogenic differentiation, in favor of fibroblastic or vasculogenic differentiation. Additionally, a lack of additional PPAR gamma expression when exposed to electrical stimulation also might indicate that the ASCs are not being induced to adipogenesis.

In terms of possible cardiac and/or osteogenic differentiation, our results will require further investigation to eludicate the effect of the electrical stimulation regime, as cells upregulated Cx-43 over the first two hours of stimulation, but also disassembled gap junctions after four hours of stimulation. Furthermore, gap junctional intercellular communication, especially through Cx-43, plays a major role in both bone [14, 15] and cardiac [16] development, and OPN gene expression is upregulated at two hours and downregulated after four hours of stimulation.

C. Future Work

The methods used here might provide the basis for a drug-free and cytokine-free method of pre-commitment of these cells. Further work is necessary to evaluate the phenotypic changes the cells undergo in the presence of electrical stimulation, and correlate the regime of stimulation with cell proliferation, differentiation and ion channel expression. Electrical stimulation has been a valuable tool for directing cellular organization, where pulsatile fields are used to engineer structured cardiac muscle constructs with enhanced cell alignment and functional connections [18]. Interestingly, this study shows that DC currents resulted in disassembly of connexons and actin fibers, concurrent with cell alignment and elongation. Therefore, treating the cells with actin antagonists inhibiting dynamic microfilaments [2] or gap junctional blockers [18], or studying cell behavior after cessation of electrical stimulation might be interesting directions of research.

Moreover, given the motility of these cells as they change morphology, we speculate that gap junctional rearrangement and cell density might play an important role in the transduction of the electric field stimulus, and cell realignment might be a way to mitigate effects from the applied electric fields. Longer experiments may reveal the steady-state cell responses to the DC field in terms of re-established cell-cell communications and reorganization.

Furthermore, the mechanism of transduction of the electrical signal to the cells is likely via ion channels, and several types have been found to be present in undifferentiated hASCs: channels for a delayed rectifier-like K+ current, a Ca2+-activated K+ current, a transient outward K current, and also a TTX-sensitive transient inward sodium current [17]. An interesting area for future work might be to investigate which of these ion channels are involved in the transduction of different regimes of electrical stimulus. Thorough characterization of heASCs is another important area of future work. The ability to modulate cardiac cell alignment and connectivity would be a valuable tool for tissue engineering applications.

ACKNOWLEDGMENT

The authors would like to thank Dr. Clark Hung for his expert guidance with bioreactor design, Keith Yeager for his technical help and advice, Dr. Timothy Martens and Amandine Godier for their help with harvesting human epicardium, and Robert Maidhof with help reviewing the manuscript. This work was funded by NIH (grants P41 EB002520 and R01 HL076485 to GVN) and by the Columbia University Presidential Fellowship (to NT).

REFERENCES

[1] Levin, M.: 'Motor protein control of ion flux is an early step in embryonic left–right asymmetry', BioEssays 2003, 25:, pp. 1002-1010

[2] Finkelstein, E., Chang, W., Chao, P.H.G., Gruber, D., Minden, A., Hung, C.T., and Bulinski, J.C.: 'Roles of microtubules, cell polarity and adhesion in electric-field-mediated motility of 3T3 fibroblasts', J Cell Sci, 2004, 117, (8), pp. 1533-1545

[3] Chao, P.-H.G., Roy, R., Mauck, R.L., Liu, W., Valhmu, W.B., and Hung, C.T.: 'Chondrocyte Translocation Response to Direct Current Electric Fields', Journal of Biomechanical Engineering, 2000, 122, (3), pp. 261-267

[4] Ferrier, J., Ross, S.M., Kanehisa, J., and Aubin, J.E.: 'Osteoclasts and osteoblasts migrate in opposite directions in response to a constant electrical field', J. Cell. Physiol., 1986, 129, (3), pp. 283-288

[5] Gruler, H., and Nuccitelli, R.: 'Neural crest cell galvanotaxis: new data and a novel approach to the analysis of both galvanotaxis and chemotaxis', Cell Motil. Cytoskeleton, 1991, 19, (2), pp. 121-133

[6] Nishimura, K.Y., Isseroff, R.R., and Nuccitelli, R.: 'Human keratinocytes migrate to the negative pole in direct current electric fields comparable to those measured in mammalian wounds', J. Cell Sci., 1996, 109, (Pt 1), pp. 199-207

[7] Soong, H.K., Parkinson, W.C., Bafna, S., Sulik, G.L., and Huang, S.C.: 'Movements of cultured corneal epithelial cells and stromal fibroblasts in electric fields', Invest. Ophthalmol. Vis. Sci., 1990, 31, (11), pp. 2278-2282

[8] Zuk, P.A., Zhu, M., Mizuno, H., Huang, J., Futrell, J.W., Katz, A.J., Benhaim, P., Lorenz, H.P., and Hedrick, M.H.: 'Multilineage Cells from Human Adipose Tissue: Implications for Cell-Based Therapies', Tissue Eng, 2001, 7, (2), pp. 211-228

[9] Tandon, N., Marsano, A., Maidhof, R., Numata, K., Montouri-Sorrentino, C., Cannizzaro, C., and Vunjak-Novakovic, G.: 'Surface-Patterned Indium Tin Oxide Electrodes for Cardiac Tissue Engineering with Electrical Stimulation', Submitted, 2009

[10] Park, H., Marsano, A., Tandon, N., Eames, E., and Cannizzaro, C.: 'Differentiation of Adipose-derived Stem Cells in an Applied Pulsatile Electric Field', Submitted, 2009

[11] Tandon, N., Cannizzaro, C., Chao, P.-H.G., Maidhof, R., Marsano, A., Au, H.T.H., Radisic, M., and Vunjak-Novakovic, G.: 'Electrical stimulation systems for cardiac tissue engineering', Nat. Protocols, 2009, 4, (2), pp. 155-173

[12] Zhao, M., Song, B., Pu, J., Wada, T., Reid, B., Tai, G., Wang, F., Guo, A., Walczysko, P., Gu, Y., Sasaki, T., Suzuki, A., Forrester, J.V., Bourne, H.R., Devreotes, P.N., McCaig, C.D., and Penninger, J.M.: 'Electrical signals control wound healing through phosphatidylinositol-3-OH kinase-[gamma] and PTEN', Nature, 2006, 442, (7101), pp. 457-460

[13] Song, B., Gu, Y., Pu, J., Reid, B., Zhao, Z., and Zhao, M.: 'Application of direct current electric fields to cells and tissues in vitro and modulation of wound electric field in vivo', Nat. Protocols, 2007, 2, (6), pp. 1479-1489

[14] Minkoff, R., Rundus, V., Parker, S., Hertzberg, E., Laing, J., and Beyer, E.: 'Gap junction proteins exhibit early and specific expression during intramembranous bone formation in the developing chick mandible', Anatomy and Embryology, 1994, 190, (3), pp. 231-241

[15] Ricardo A. Rossello, D.H.K.: 'Gap junction intercellular communication: A review of a potential platform to modulate craniofacial tissue engineering', Journal of Biomedical Materials Research Part B: Applied Biomaterials, 2009, 88B, (2), pp. 509-518

[16] Moore, J.C., Tsang, S.-Y., Rushing, S.N., Lin, D., Tse, H.F., Chan, C.W.Y., and Li, R.A.: 'Functional consequences of overexpressing the gap junction Cx43 in the cardiogenic potential of pluripotent human embryonic stem cells', Biochemical and Biophysical Research Communications, 2008, 377, (1), pp. 46-51

[17] Bai, X., Ma, J., Pan, Z., Song, Y.-H., Freyberg, S., Yan, Y., Vykoukal, D., and Alt, E.: 'Electrophysiological properties of human adipose tissue-derived stem cells', Am J Physiol Cell Physiol, 2007, 293, (5), pp. C1539-1550

[18] Radisic, M., Park, H., Shing, H., Consi, T., Schoen, F.J., Langer, R., Freed, L.E., and Vunjak-Novakovic, G.: 'Functional assembly of engineered myocardium by electrical stimulation of cardiac myocytes cultured on scaffolds', Proc. Natl. Acad. Sci. U. S. A., 2004, 101, (52), pp. 18129-18134

[19] Bai, X., Pinkernell, K., Song, Y.-H., Nabzdyk, C., Reiser, J., and Alt, E.: 'Genetically selected stem cells from human adipose tissue express cardiac markers', Biochemical and Biophysical Research Communications, 2007, 353, (3), pp. 665-671